Open System Assessment of Corrosion Rate of Aluminum-Manganese Alloy in Sea Water Environment Based on Exposure Time and Alloy Weight Loss

C. I. Nwoye[1], N. E. Idenyi[2], F. Asuke*[3], E. M. Ameh[4]

[1]*Department of Metallurgical and Materials Engineering, Nnamdi Azikiwe University, Awka, Nigeria.*
[2]*Department of Industrial Physics, Ebonyi State University, Abakaliki, Nigeria.*
[3]*Department of Metallurgical and Materials Engineering, Ahmadu Bello University, Zaria, Nigeria.*
[4]*Department of Metallurgical and Materials Engineering, Enugu State University of Science & Technology, Enugu, Nigeria*

Abstract

Open system corrosion rate of aluminium-manganese (Al-Mn) alloy in sea water environment was assessed based on the alloy weight loss and exposure time. A model was derived and used as a tool for the assessment. It is made up of a quadratic and natural logarithmic function. The validity of the model is rooted on the core expression: $1.0126 \times 10^{-2} \, C_R = \alpha^2 - 11.9538 \times 10^{-2} \, \alpha + 4.5059 \times 10^{-4} \ln\gamma + 6.1968 \times 10^{-3}$ where both sides of the expression are correspondingly approximately equal. Statistical analysis of model-predicted, regression-predicted and experimentally evaluated corrosion rates for each value of exposure time and alloy weight loss considered shows a standard error of 0.0657, 0.0709 & 0.0715 % and 0.0190 & 2.83×10^{-5} & 0.0068 % respectively. The resultant depth of corrosion penetration as predicted by derived model, regression model and obtained from experiment are 0.0102, 0.01 and 0.0112 mm respectively, while the corrosion rate per unit weight loss of the alloy as predicted by derived model, regression model and obtained from experiment are 7.7830, 7.6774 and 8.5777 mm/yr/g respectively. The maximum deviation of the model-predicted alloy corrosion rates from the corresponding experimental values is less than 27%.

Keywords: Open System Assessment, Corrosion Rate, Al-Mn Alloys, Sea Water, Exposure Time, Alloy Weight Loss.

Introduction

In aggressive environments, the stability of metals or alloys has been reported [1] to basically depend on the protective properties of organic or inorganic films as well as on the layer of corrosion products. The researchers concluded that the ability of films to act as controlling barriers against different kinds of corrosion attack is dependent on film properties such as chemical composition, adhesion, conductivity, solubility, morphology and hygroscopicity. Past studies [2,3] reported that the highlighted characteristic of films in turn depends on environmental variables such as atmospheric conditions, type and amount of pollutants as well as wet-dry cycle, the chemical composition and metallurgical history of the metals or alloys and physicochemical properties of coating.

The applicability of aluminium and its alloys in many industries have been attributed to their high strength-to-weight ratios, good corrosion resistance, excellent workability and high thermal/electrical conductivity [4-14]. However, the ability of aluminium and its alloy to resist corrosion attack in aggressive environment have been reported to be poor and insufficient [15]. In recent years, various methods, have been devised to address some limitations of the alloy in the areas of alloying addition [16], thermal treatment [17-20], and composite/nano-composite formation [21,22]. Also, corrosion resistance of aluminium and its alloys have been investigated in various environments using inhibitors [8,9, 23-27]. Some synthetic corrosion inhibitors have been identified to be toxic and non ecologically-friendly [28,29]. Use of ecologically-friendly and non-toxic corrosion inhibitors have also received focus among researchers in recent time. The use of plant extract and oils, otherwise known as green corrosion inhibitors has gained wide acceptablity and applicability due to their availability, non toxicity and renewable source of materials for wide range of corrosion control [14,30]. The non-toxic nature of tiger nut oil has been investigated [31-35] with the view to ascertaining its applicability to corrosion inhibition.

Al-Mn alloys have been reported to be susceptible to corrosion attack because of the presence of moisture and oxygen in the atmosphere [36]. The corrosion of this alloy is due to the strong affinity aluminium has for oxygen which results to its oxidation and subsequent formation of oxide film. Ekuma et al., [37] reported that with time, this film becomes passive to further oxidation and stable in aqueous media when the pH is between 4.0 and 8.5. It is important to state that the passive films can break and fall of, hence exposing the surface of the alloy to further corrosion.

The corrosion rate of Al-Mn alloy in atmospheric environment has been predicted based on the initial weights of the alloy (γ) and its exposure times (α) [38]. The predictive analysis was carried out using a derived model expressed as:

$$\beta = -3.4674\ \alpha^2 + 0.3655\alpha - 0.0013\gamma^2 + 0.007\gamma - 0.0031 \qquad (1)$$

The validity of the two-factorial quadratic model is rooted on the core expression $0.2884\ \beta = -\alpha^2 + 0.1054\alpha - 3.7489 \times 10^{-4}\ \gamma^2 + 2.0186 \times 10^{-3}\gamma - 8.9396 \times 10^{-4}$ where both sides of the expression are correspondingly approximately equal. Statistical analysis of model-predicted and experimentally evaluated corrosion rates as well as depth of corrosion penetration for each value of alloy initial weight and exposure time considered show standard errors of 0.0014 and 0.0015 % as well as 9.48×10^{-4} and 8.64×10^{-4} %, respectively. Corrosion rate per unit initial weight of exposed alloy as predicted by derived model and obtained from experiment are 1.8421 and 1.6316 (mm/yr) kg^{-1} respectively. Similarly, between exposure time: 0.0192 - 0.0628 yr, the depth of corrosion penetration on the exposed alloy as predicted by derived model and obtained from experiment are 1.5260×10^{-4} and 1.3516×10^{-4} mm respectively. The maximum deviation of the model-predicted corrosion penetration rate (from the corresponding experimental value) is less than 11%.

The aim of this work is to ascertain the predictability of aluminium-manganese alloy corrosion rate based on its weight loss and exposure time in sea water environment. The method adopted for the research is the weight loss technique. Earlier research work on Al-Mn alloy corrosion rate [38] predicted the alloy corrosion rate in atmospheric environment devoid of water. However, the proposed work aims at predicting same alloy corrosion rate in sea water environment. Furthermore, the present work is concerned with the weight loss of the alloy following corrosion attack while past research [38] considered the initial weight of the alloy before corrosion attack.

2. Materials and methods

The method adopted for this phase of the research is the weight loss technique. Materials used for the experiment are aluminium of 99% purity and pure granulated manganese, acetone, sodium chloride, distilled water, beakers and measuring cylinders. The equipment used were lathe machine, drilling machine, crucible furnace and analytical digital weighing machine.

2.1 Specimen preparation and experimentation

Computation for each of the Al-Mn alloy compositions was carefully worked out, and 500g of the alloying materials charged into the crucible furnace. The molten alloy was cast into rods and allowed to cool in air (at room temperature). The cooled rods were machined to 20mm diameter, cut into test samples 10 mm long and weighed. Each cut sample (coupon) was drilled with 5mm drill bit to provide hole for the suspension of the strings. The surface of each of the test coupons was thoroughly polished with emery cloth according to ASM standards (ASM E407). The test coupons were exposed to the sea water and withdrawn after a given period of time. The withdrawn coupons were washed with distilled water, cleaned with acetone and dried in open air before weighing. This weight was subtracted from its initial weight to determine the weight loss.

3. Results and discussion

Table 1 shows the result of the effects of exposure time and Al-Mn alloy weight loss on the alloy corrosion rate.

Table 1: Variation of corrosion rate of Al-Mn alloy with its exposure time and weight loss

C_R (mm/yr)	(α) (hrs)	(γ) (g)
0.3024	168	0.0378
0.1753	240	0.0222
0.0048	336	0.0012
0.0083	450	0.0029
0.0099	504	0.0037

3.2 Model formulation

Experimental data obtained from the research work were used for this work. Computational analysis of these data shown in Table 1 using a soft ware (C-NIKBRAN) [39], gave rise to Table 3 which indicate that;

$$K\,C_R = \alpha^2 - N\alpha + S\,\ln\gamma + S_e \qquad (2)$$
Introducing the values of K, N, S, and S_e into equation (2)

$$1.0126 \times 10^{-2}\,C_R = \alpha^2 - 11.9539 \times 10^{-2}\,\alpha + 4.5059 \times 10^{-4}\,\ln\gamma + 6.1968 \times 10^{-3} \qquad (3)$$

$$C_R = \frac{\alpha^2 - 11.9539 \times 10^{-2}\,\alpha + 4.5059 \times 10^{-4}\,\ln\gamma + 6.1968 \times 10^{-3}}{1.0126 \times 10^{-2}} \qquad (4)$$

$$C_R = 98.76\,\alpha^2 - 11.8051\alpha + 0.0445\,\ln\gamma + 0.612 \qquad (5)$$

Where

$K = 1.0126 \times 10^{-2}$; Overall Al-Mn alloy-sea water temperature interaction factor (determined using C-NIKBRAN [39])

$N = 11.9539 \times 10^{-2}$; First order alloy degradability Coefficient (determined using C-NIKBRAN [39])

$S = 4.5059 \times 10^{-4}$; Film solubility-adhesion ratio in sea water (determined using C-NIKBRAN [39])

$S_e = 6.1968 \times 10^{-3}$: Al-Mn alloy oxidation coefficient (determined using C-NIKBRAN [39])

C_R = Corrosion rate (mm/yr)

(α) = Exposure time (yr)

(γ) = Alloy weight loss (g)

The derived model is two-factorial in nature because it is a constituent of two input process factors: alloy weight loss and exposure time. This implies that the predicted corrosion rate for the Al-Mn alloy in sea water environment is dependent on just two factors: alloy weight loss and exposure time

3.3 Boundary conditions

Range of exposed time considered: 0.0192 - 0.0575 yrs (168-504 hrs). Alloy weight loss range considered: 0.0012-0.0378 g, aerobic environment to enhance Al-Mn alloy oxidation (since the sea water contains oxygen. At the bottom of the exposed alloy, a zero gradient for the gas scalar are assumed. The exposed alloy is stationary. The sides of the solid are taken to be symmetries.

3.4 Initial conditions

Exposure of solid Al-Mn alloy to sea water environment, the sea water is assumed to be affected by unwanted dissolved gases. Purity of aluminium used: 99%. Concentration of manganese addition: 1 %.

Table 2: Variation of corrosion rate of Al-Mn alloy with its evaluated exposure time and weight loss

C_R (mm/yr)	(α) (yrs)	(γ) (g)
0.3024	0.0192	0.0378
0.1753	0.0274	0.0222
0.0048	0.0384	0.0012
0.0083	0.0514	0.0029
0.0099	0.0575	0.0037

Table 3: Evaluation and variation of model forming mathematical expressions

(α^2)	$11.9539 \times 10^{-2}\,\alpha$	$4.5059 \times 10^{-4}\,\ln\gamma$	6.1968×10^{-3}
0.3686×10^{-3}	2.0237×10^{-3}	0.000049×10^{-3}	6.1968×10^{-3}
0.7508×10^{-3}	2.8880×10^{-3}	0.000055×10^{-3}	6.1968×10^{-3}
1.4746×10^{-3}	4.0474×10^{-3}	0.000064×10^{-3}	6.1968×10^{-3}
2.6420×10^{-3}	6.6191×10^{-3}	0.000066×10^{-3}	6.1968×10^{-3}
3.3063×10^{-3}	8.0842×10^{-3}	0.000068×10^{-3}	6.1968×10^{-3}

Table 4: Variation of $1.0126 \times 10^{-2}\, C_R$ with $\alpha^2 - 11.9539 \times 10^{-2}\, \alpha + 4.5059 \times 10^{-4}\, \ln\gamma + 6.1968 \times 10^{-3}$

$1.0126 \times 10^{-2}\, C_R$	$\alpha^2 - 11.9539 \times 10^{-2}\, \alpha + 4.5059 \times 10^{-4}\, \ln\gamma + 6.1968 \times 10^{-3}$
3.0621×10^{-3}	2.7944×10^{-3}
1.7751×10^{-3}	1.9565×10^{-3}
0.0486×10^{-3}	0.0507×10^{-3}
0.0840×10^{-3}	0.0617×10^{-3}
0.1003×10^{-3}	0.1067×10^{-3}

The validity of the model is strongly rooted on the core model equation: $1.0126 \times 10^{-2}\, C_R = \alpha^2 - 11.9539 \times 10^{-2}$ $\alpha + 4.5059 \times 10^{-4}\, \ln\gamma + 6.1968 \times 10^{-3}$ (equation (3)) where both sides of the equation are correspondingly approximately equal. Computed values at the left and right hand sides of Table 4 complement this position. Furthermore, the derived model was validated by comparing the corrosion rate predicted by the model and that obtained from the experiment. This was done using various analytical techniques.

3.1 Computational Analysis
Computational analysis of the experimental and model-predicted corrosion rate per unit weight loss and corrosion penetration depth were carried out to ascertain the degree of validity of the derived model. The idea is to compare the model-predicted corrosion penetration depth with that obtained from experimental result as a way of checking how close the model prediction is to experimental results. This was done by comparing the depth of corrosion penetration obtained by calculations involving experimental results, and predicted directly by the model.

Corrosion rate per unit weight loss on Al-Mn alloy during the period of exposure in the sea water environment C_{Wloss} (mm/yr/g) was calculated from the equation;

$$C_{Wloss} = \Delta C_{Wloss} / \Delta\gamma \qquad (6)$$

Equation (6) is detailed as

$$C_{Wloss} = C_{R2} - C_{R1} / \gamma_2 - \gamma_1 \qquad (7)$$

Where
ΔC_{Wloss} = Change in the corrosion rates $(C_{R2} - C_{R1})$ at two alloy weight loss values: γ_2, γ_1
  $\Delta\gamma$ = Change in the two alloy weight loss values: $\gamma_2 - \gamma_1$
Furthermore, substituting experimental results of points (0.0378, 0.3024) and (0.0037, 0.0099) for (γ_1, C_{R1}) and (γ_2, C_{R2}) respectively (as in Fig. 1) and substituting them into equation (7), gives a slope: 8.5777 mm/yr g^{-1} as the corrosion rate per unit weight loss on the alloy during the actual corrosion process. Also, substitution of the model-predicted results of points (0.0378, 0.2759) and (0.0037, 0.0105) for (γ_1, C_{R1}) and (γ_2, C_{R2}) respectively (as in Fig. 2), into equation (7) gives the slope as the corrosion rate per unit weight loss on the alloy as 7.7820 mm/yr g^{-1}. On the other hand, on substitution of regression-model predicted results of points (0.0378, 0.2836) and (0.0037, 0.0218) for (γ_1, C_{R1}) and (γ_2, C_{R2}) respectively (as in Fig. 3), into equation (7) the slope; corrosion rate per unit weight loss on the alloy was evaluated as 7.6774 mm/yr g^{-1}.

The depth of corrosion penetration on Al-Mn alloy during the period of exposure in the sea water environment C_D (mm) was calculated from the equation;

$$C_D = \Delta C_R \times \Delta\alpha \qquad (8)$$

Where
ΔC_R = Change in the corrosion rates $(C_{R2} - C_{R1})$ within a range of exposure time: $\alpha_1 - \alpha_2$.
 $\Delta\alpha$ = Change in the alloy exposure time α_2, α_1

Considering experimental results of points (0.0192, 0.3024) and (0.0575, 0.0099) for (α_1, C_{R1}) and (α_2, C_{R2}) respectively (as in Fig. 4) and substituting them into equation (8), gives – 0.0112 mm as the depth of corrosion penetration on the alloy during the actual corrosion process. Also similar plot (as in Fig. 5) using model-predicted results of points (0.0192, 0.2759) and (0.0575, 0.0105) for (α_1, C_{R1}) and (α_2, C_{R2}) respectively, and substituting them into equation (8) gives the depth of corrosion penetration on the alloy as - 0.0102 mm. This is the model-predicted depth of corrosion penetration on the alloy. Similarly, using regression-model predicted results of points (0.0192, 0.2836) and (0.0575, 0.0218) for (α_1, C_{R1}) and (α_2, C_{R2}) respectively (as in Fig. 6), and substituting them into equation (8) gives the depth of corrosion penetration on the alloy as - 0.01 mm. These plots show the proximity of model-predicted results to regression model-predicted (from standard model) and experimental result considering their respective slopes and coefficients. The closeness of these results imputes validity to the derived model.
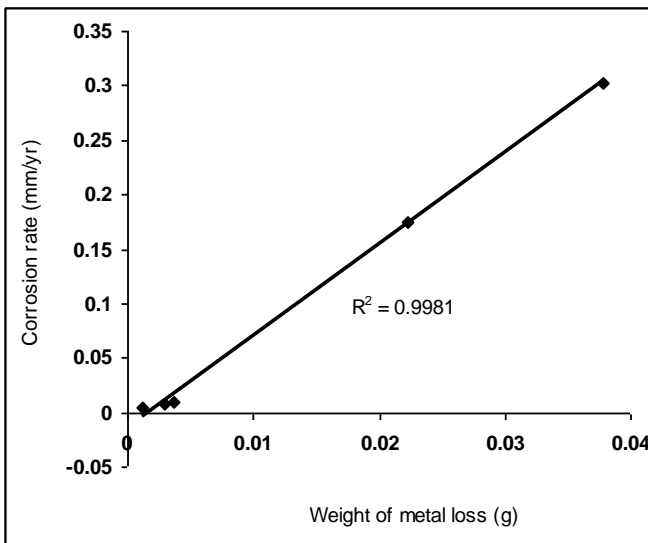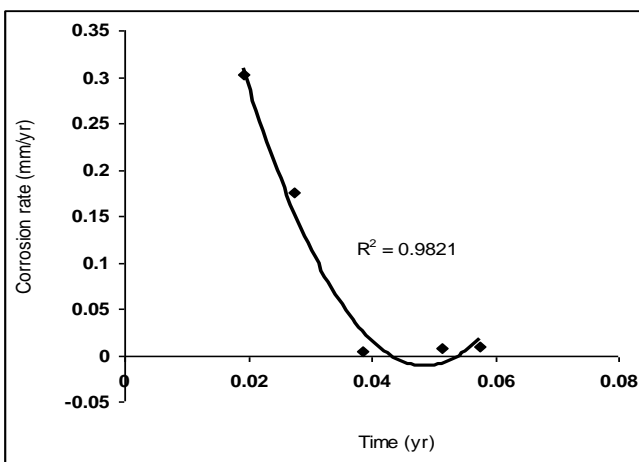
Figure 1: Coefficient of determination between corrosion rate and alloy weight loss as obtained from the experiment
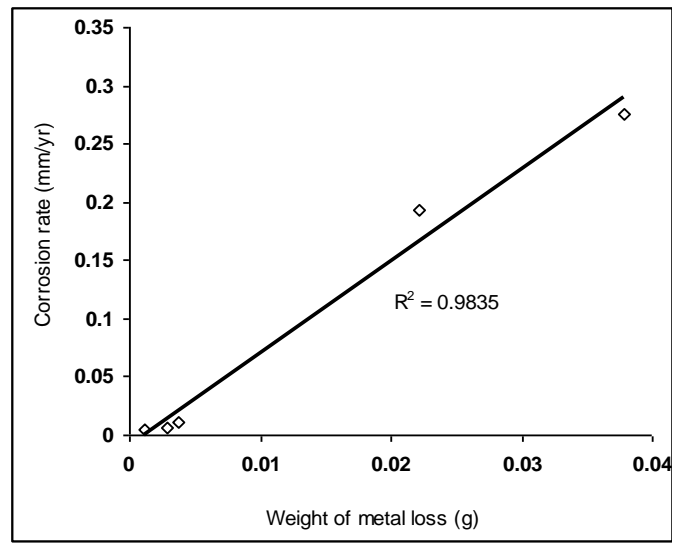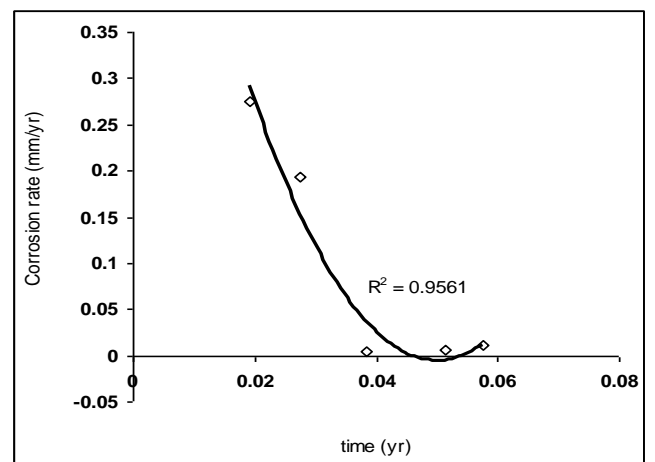

Figure 2: Coefficient of determination between corrosion rate and alloy weight loss as predicted by derived model.
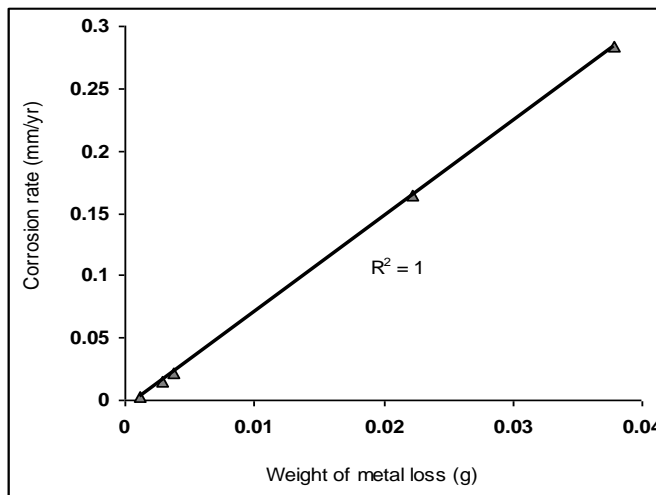
Figure 3: Coefficient of determination between corrosion rate and alloy weight loss as predicted by regression model.

Figure 4: Coefficient of determination between corrosion rate and alloy exposure time as obtained from the experiment

Figure 5: Coefficient of determination between corrosion rate and alloy exposure time as predicted by derived model

The negative signs preceding the magnitudes of the depth of corrosion penetration do not indicate that the depth of the penetration is negative, but that the magnitude of the corrosion rate just before penetration of the alloy

dropped during the penetration process. As a result, the change in the corrosion rates at the onset and end of penetration is negative. Based on the foregoing, the negative sign is neglected.

3.2. Statistical analysis
Statistical analysis of model-predicted, regression-model predicted and experimentally evaluated corrosion rates indicates that the standard error (STEYX) in predicting the corrosion rate for each value of alloy exposure time and weight loss considered are 0.0657, 0.0709 & 0.0715 % and 0.0190 & 2.83 x 10^{-5} & 0.0068 % respectively. The standard error was evaluated using a Microsoft Excel 2003 [9]. The correlations between corrosion rate and alloy weight loss as well as corrosion rate and exposure time as obtained from derived model, regression model and experimental results were calculated. This was done by considering the coefficients of determination R^2 from Figs. 1-6, using the equation;

$$R = \sqrt{R^2} \tag{9}$$
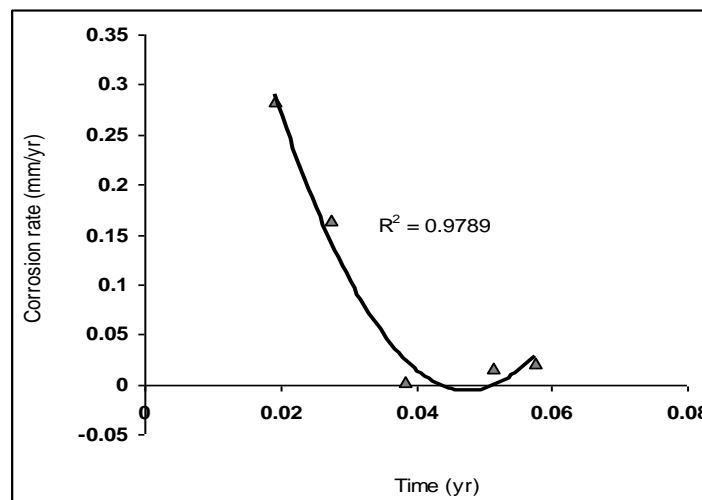
Figure 6: Coefficient of determination between corrosion rate and alloy exposure time as predicted by regression model

The evaluated correlations are shown in Tables 4 and 5. The model was also validated by comparing its results of evaluated correlations between corrosion rate and alloy weight loss as well as corrosion rate and exposure time with that evaluated using experimental and regression model-predicted results. Tables 4 show that the correlation result from experiment, derived model and regression model are in proximate agreement.

Table 4: Comparison of the correlations between corrosion rate & exposure time as well as corrosion rate & alloy weight loss as evaluated from experimental (ExD), derived model (MoD) and regression-model (MoR) predicted results

| Analysis	Based on alloy exposure time			Based on alloy weight loss		
	ExD	MoD	MoR	ExD	MoD	MoR
CORREL	0.9910	0.9778	0.9894	0.9990	0.9917	1.0000

3.3 Graphical Analysis
Comparative graphical analysis of Figs. 7 and 8 shows very close alignment of the curves from derived model and experiment. Figs. 9 and 10 also indicate a close alignment of curves from derived model and regression-model predicted results as well as experimental results of corrosion rate. It is strongly believed that the degree of alignment of these curves is indicative of the proximate agreement between ExD, MoD and MoR predicted results.

Comparison of derived model with standard model
The validity of the derived model was further verified through application of the Regression Model [9] in predicting the trend of the experimental results for the values of alloy weight loss and exposure time considered. Results predicted by the regression model was plotted; corrosion rate against alloy weight loss and exposure time respectively along with results from the experiment and derived model to analyze its spread and trend relative to results from experiment and derived model.

Comparative analysis of Figs. 9 and 10 shows very close alignment of curves and significantly similar trend of data point's distribution for experimental (ExD), derived model-predicted (MoD) and Regression Model (MoR) predicted results of corrosion rate.
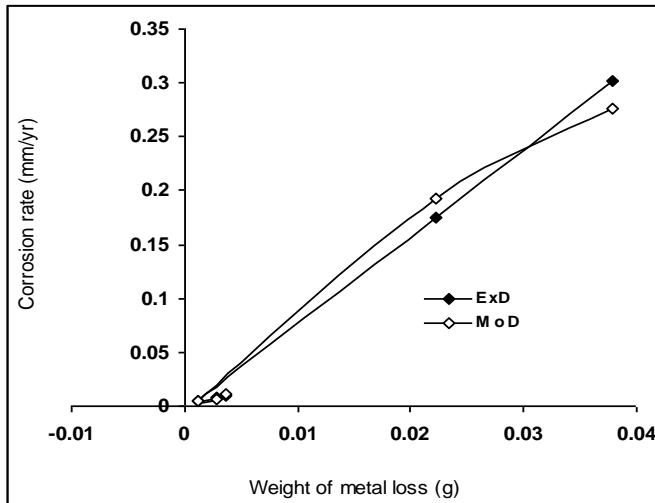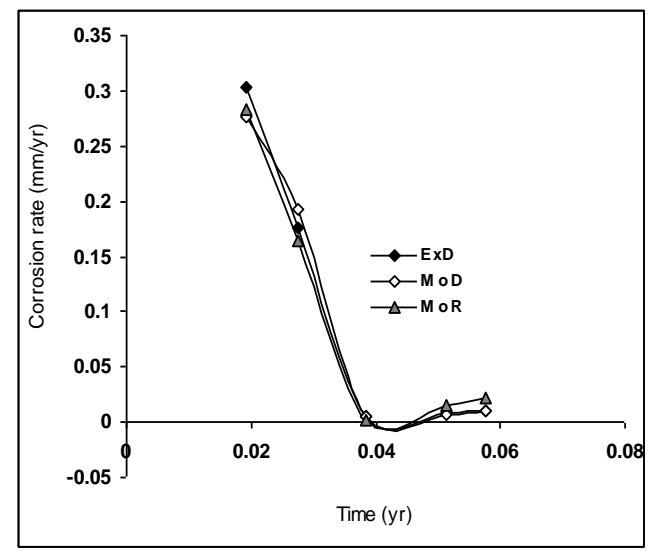

Figure 7: Comparison of the corrosion rate (relative to alloy weight loss) as obtained from experiment and derived model.
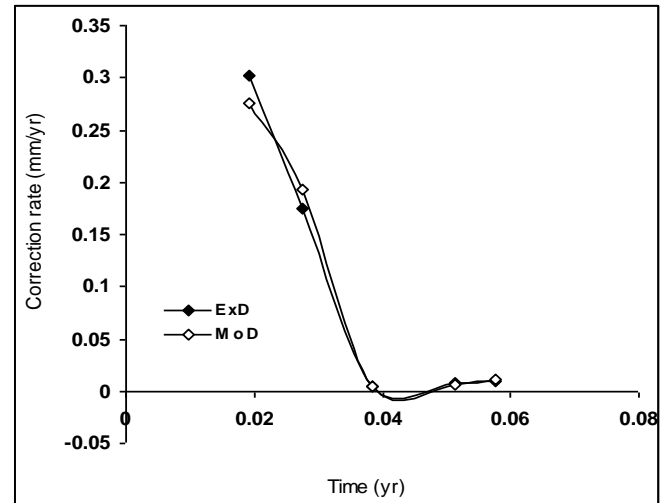
Figure 8: Comparison of the corrosion rate (relative to alloy exposure time) as obtained from experiment and derived model.
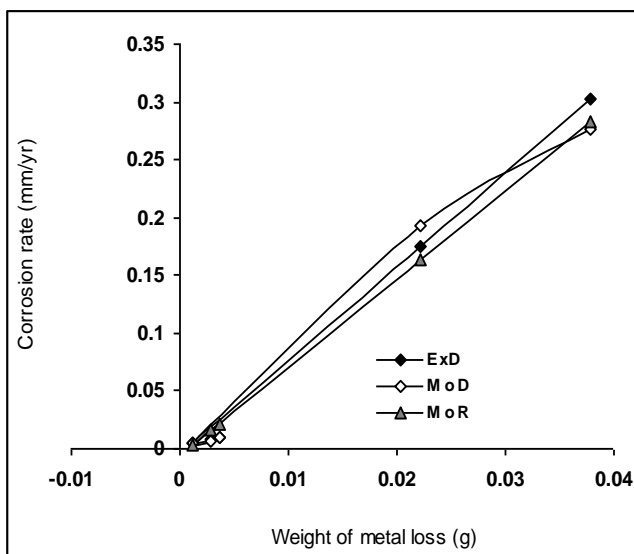
Figure 9: Comparison of the corrosion rate (relative to alloy weight loss) as obtained from experiment, derived model and regression model.

Figure 10: Comparison of the corrosion rate (relative to alloy exposure time) as obtained from experiment, derived model and regression model

3.4 Deviational Analysis
Deviational analysis examines the percent level of discrepancies in the model-predicted results on comparing them with results from experiment. Comparative analysis of corrosion rate from the experiment and derived model revealed deviations on the part of the model-predicted values relative to values obtained from the experiment. This is attributed to the fact that the surface properties of the alloy and the physiochemical interaction between the alloy and corrosion induced agents (in the sea water) were not considered during the model formulation. This necessitated the introduction of correction factor, to bring the model-predicted corrosion rate to those of the corresponding experimental values.

Deviation (Dn) of model-predicted corrosion rate from that of the experiment [7] is given by

$$De = \left[\frac{Pr - Er}{Er} \right] \times 100 \qquad\qquad (10)$$

Correction factor (Cr) is the negative of the deviation i.e
$$Cf = -De \tag{11}$$
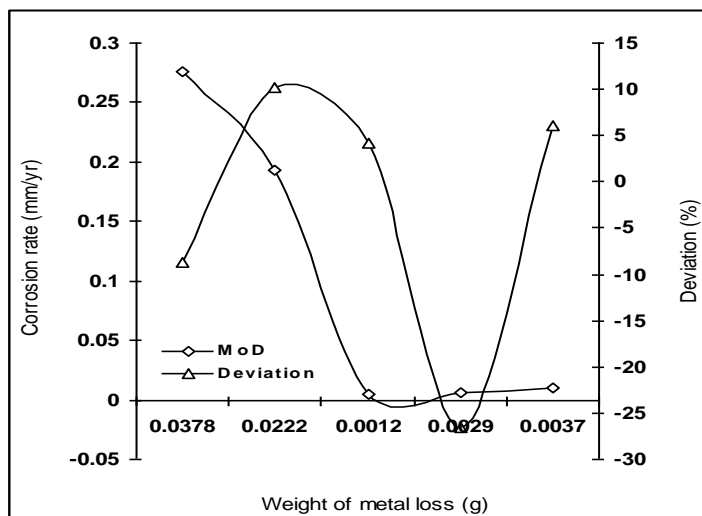Therefore

$$Cf = - \left[\frac{Pr - Er}{Er}\right] \times 100 \tag{12}$$

Where

   Pr = Model-predicted corrosion rate (mm/yr)

   Er = Corrosion rate obtained from experiment (mm/yr)

   Cf = Correction factor (%)
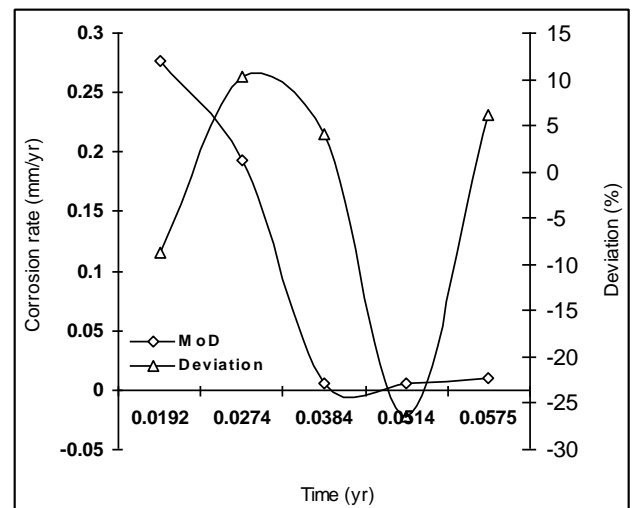
   De = Deviation (%)

Introduction of the corresponding values of Cf from equation (12) into the model gives exactly the corresponding experimental corrosion rate.

Figure 11: Variation of model-predicted corrosion rate (relative to alloy weight loss) with its associated deviation from experimental values
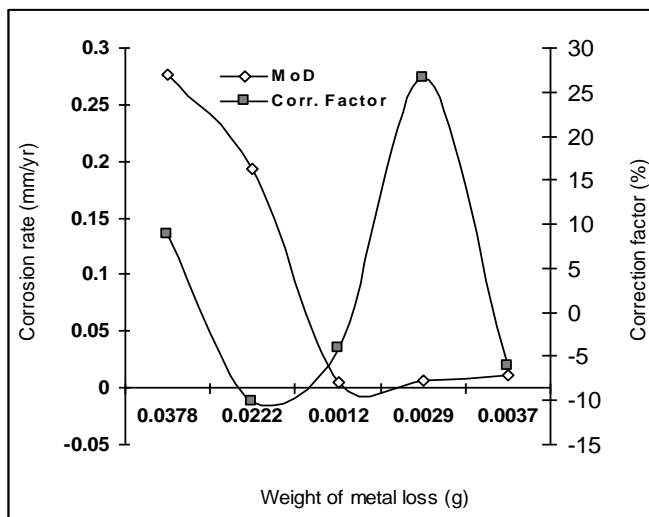
Figure 12: Variation of model-predicted corrosion rate (relative to alloy weight loss) with its associated correction factor

Figure 13: Variation of model-predicted corrosion rate (relative to alloy exposure time) with its associated deviation from experimental values

Figs. 11 and 13 show that the maximum deviation of the model-predicted corrosion rate from the corresponding experimental values is less than 27% and quite within the acceptable deviation limit of experimental results. These figures show that least and highest magnitudes of deviation of the model-predicted corrosion rate (from

the corresponding experimental values) are + 4.17 and -26.51% which corresponds to exposure times: 0.0384 and 0.0514 yr, alloy weight loss; 0.0012 and 0.0029 g and corrosion rates between; 0.005 and 0.0061 mm/yr respectively.

Comparative analysis of Figs. 11-14 indicates that the orientation of the curve in Figs. 12 and 14 is opposite that of the deviation of model-predicted corrosion rate (Figs.11 and 13). This is because correction factor is the negative of the deviation as shown in equations (11) and (12). It is believed that the correction factor takes care of the effects of the surface properties of the alloy which were not considered during the model formulation. Figs. 12 and 14 indicate that the least and highest magnitudes of correction factor to the model-predicted corrosion rate are − 4.17 and + 26.51 % which corresponds to exposure times: 0.0384 and 0.0514 yr, alloy weight loss; 0.0012 and 0.0029 g and corrosion rates between; 0.005 and 0.0061 mm/yr respectively.

It is important to state that the deviation of model predicted results from that of the experiment is just the magnitude of the value. The associated sign preceding the value signifies that the deviation is deficit (negative sign) or surplus (positive sign).
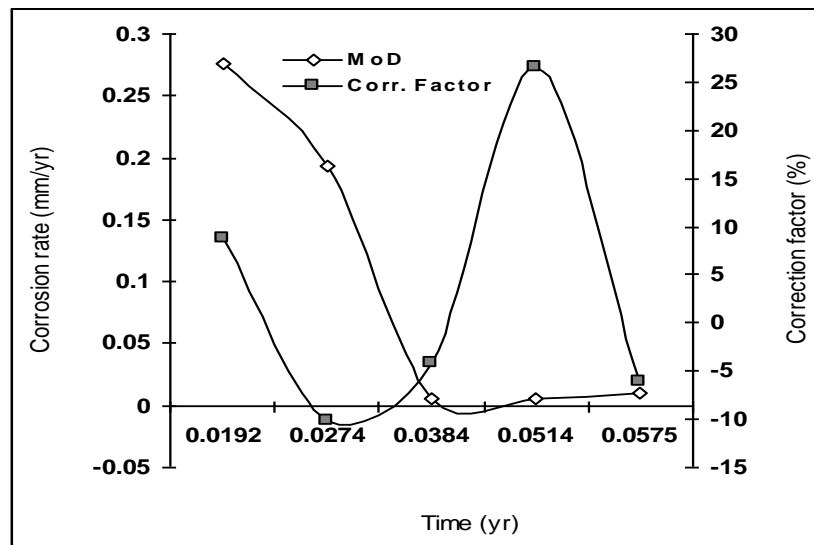
Figure 14: Variation of model-predicted corrosion rate (relative to alloy exposure time) with its associated correction factor

It is important to state that the large swing in the correction factor resulted from equal magnitude of swing coming from deviation of model-predicted results (from those of the experiment). The swing in deviation resulted from a sharp increase in the weight loss at a corresponding sharp increase in the exposure time. These sharp increases actually affected the corrosion rate sharply during the experiment because the surface properties of the alloy and the physiochemical interaction between the alloy and corrosion induced agents (in the sea water) played their roles. However, the derived model predicted its results directly without considering these constraints.

Conclusion

Aluminium-manganese (Al-Mn) alloy exposure time has been predicted based on its as-cast weight and corrosion rate in sea water environment. The validity of the derived model is rooted on the core expression: $1.0126 \times 10^{-2} C_R = \alpha^2 - 11.9538 \times 10^{-2} \alpha + 4.5059 \times 10^{-4} \ln \gamma + 6.1968 \times 10^{-3}$ where both sides of the expression are correspondingly approximately equal. Statistical analysis of model-predicted, regression-predicted and experimentally evaluated corrosion rates for each value of exposure time and alloy weight loss considered shows a standard error of 0.0657, 0.0709 & 0.0715 % and 0.0190 & 2.83 x 10^{-5} & 0.0068 % respectively. The resultant depth of corrosion penetration as predicted by derived model, regression model and obtained from experiment are 0.0102, 0.01 and 0.0112 mm respectively. Furthermore, the corrosion rate per unit weight loss of the alloy as predicted by derived model, regression model and obtained from experiment are 7.7830, 7.6774 and 8.5777 mm/yr/g respectively. Deviational analysis indicates that the maximum deviation of the model-predicted alloy corrosion rate from the corresponding experimental value is less than 27%.

References

1. Stratmann, M., Bohnenkamp, K., and Engell, W. J. *Corrosion Science*, 23(1983) 969-985.
2. Ekuma, C. E., and Idenyi, N. E. *Research Journal of Physics USA,* 1(1) (2007) 27-34.
3. Stratmann, S. G., and Strekcel, H. *Corrosion Science*, 30 (1990) 697-714.
4. Rosliza, R. Nik, W. B. W. *Current Applied Physics*, 10 (2010) 221-229.
5. Gbenebor, O. P., Abdulwahab, M., Fayomi, O. S. I., Popoola, A. P. I. *Chalcogenide Letters,* 9 (5) (2012) *201.*
6. Abdulwahab, M., Madugu, I.A., Yaro, S. A., Hassan, S. B., Popoola, A. P. I. *Materials and Design,* 32(3) (2011a) 1159.
7. Ajayi, O. O., Omotosho, O. A., Ajanaku, K. O. and Olawore. *Environmental Research Journal, 5*(4) (2011) 163.
8. Kumpawat, V. Garg, U. and Tak, R. K. *J. Ind. Council Chem.,* 26(1) (2009) 82.
9. Rosliza, R. Nora'aini, A., Nik, W. B. W. *Journal of Applied Electrochemistry*, 40 (2010) 833.
10. Metikos-Hukovic, M., Basic, R. and Grubac, Z. *Journal of Applied Electrochemistry,* 32 (2002) 35.
11. Abdulwahab, M., Madugu, I. A., Yaro, S. A., Popoola, A. P. I. *Silicon,* 4 (2) (2012a) 137.
12. Amin, M.A., Hassan, H. H., Hazzazi, O. A., Qhatani, *Journal of Applied Electrochemistry,* 38 (2008) 1589.
13. Al-Turkustani, A. M., Al-Solmi, M. M. *Journal of Asian Scientific Research,* 1(7) (2011) 346.
14. Halambek, J., Berkovic, K., Vorkapic-Furac, J. *Corrosion Science,* 52 (2010) 3978.
15. Rajasekar, A. and Ting, Y. P. *Industrial and Engineering Chemistry Research,* 50 (2011) 2040.
16. Fang Hua-Chan, Chen Kang-Hua, Zhang Zhou, Zhu Changjun. *Trans Nonferr Metals Soc China,* 18 (2008) 28.
17. Li Zhihui, Xiong Baiqing, Zhang Yongan, Zhu Baohong, Wang Feng, Liu Hongwei. *Mater. Charact.,* 494 (2008) 278.
18. Risanti, D.D, Yin M, Rivera Diazdel Castillo P.E.J, Vau der Zwang S. *Mater. Sci. Eng.,* A5 23 (2009) 99.
19. Abdulwahab, M., Madugu, I.A., Yaro, S. A., Popoola, A. P.I. *Journal of Minerals and Materials Characterization and Engineering,* 10(6) (2011b) 535.
20. Lumley, R. N, Odonnell, R. G, Gunasegaram, D. R, Givord, M. *Metall. Mater. Trans.* A 38A (2007) 2564.
21. Ali Mazahery, Mohsen Ostad Shabani. *Trans. Nonferrous Met. Soc. China*, 22 (2012) 275.
22. Sha, G., Moller, H., Stumpt, W. E., Xia, J. H., Govender, G., Ringer, S. P. Solute *Acta Materialia*, 60 (2012) 692.
23. Abdulwahab, M., Kassim, A., Bello, K. A., Gaminana, J. O. *Advanced Materials Research*, 367 (2012b) 319-325.
24. Umoren, S. A., Obot, I. B., Ebenso, E. E., Okafor, P. C. *Portugaliae Electrochemica Acta,* 26 (2008a) 267.
25. Umoren, S. A., Ebenso, E. E. *Pigment and Resin Technology,* 37 (2008b) 173.
26. Umoren, S. A., Obot, I. B., Ebenso, E. E., Okafor, P. C., Ogbode, O., Oguzie, E. E. *Anti-corrosion Methods and Materials,* 53 (2006) 277.
27. Abiola, O. K., Otaigbe, J. O. E., Kio, O. J. *Corrosion Science*, 51(2009) 1879.
28. Saji, V. S. *Corrosion Science,* 2 (2010) 6.
29. Sangeetha, M., Rajendran, S., Muthumegala, T. S., Krishnaveni. *Zastita Materijala,* 52 (2011) 3.
30. Bammou, L., Mihit, M., Salghi, R., Bouyanzer, A., Al-Deyab, S. S., Bazzi, L., Hammouti, B. *Int. J. Electrochem. Sci.,* 6 (2011) 1454.
31. Muhammad, N. O., Bamishaiye, E. I., Bamishaiye, O. M., Usman, L. A., Salawu, M.O., Nafiu, M. O. and Oloyede, O. B. *Bioresearch Bulletin*, 5 (2011) 51.
32. Yeboah, S. O., Mitei, Y. C., Ngila, J. C., Wessjohann, L., Schmidt, J. *Food Research International* (2011), doi:10.1016/j.foodres.2011.06.036.
33. Shaker, M. A., Ahmed, M. G., Amany, M. B. and Shereen, L. N. *World Applied Sciences Journal,* 7 (2) (2009) 151.
34. Belewu, M. A. and Belewu, K. Y. *International Journal of Agriculture & Biology, 9(5)* (2007) 785.
35. Kubmarawa, D., Ogunwande, I. A., Okorie, D. A., Olawore, N. O. and Kasali, A. A. *Flavour and Fragrance Journal,* 20 (2011) 640.
36. Polmear, I., J. Light Alloys. Edward Arnold Publishers Ltd. (1981).
37. Ekuma, C. E., Idenyi, N. E., and Umahi, A. E. *Journal of Applied Science,* 7(2) (2007) 237-241.
38. Nwoye, C. I., Idenyi, N. E., and Odo, J. U. *Nig. J. Mat. Sci. Eng.*, 3(1) (2012) 8-14.
39. Nwoye, C. I. C-NIKBRAN-Data Analytical Memory (Software). (2008).

(2013) ; http://www.jmaterenvironsci.com